photonics

MDPI

Communication

Quantum State Tomography in Nonequilibrium Environments

Haonan Chen [1], Tao Han [1], Mingli Chen [1], Jing Ren [1,*], Xiangji Cai [1,*], Xiangjia Meng [2], Yonggang Peng [3]

[1] School of Science, Shandong Jianzhu University, Jinan 250101, China
[2] School of Information Engineering, Shandong Youth University of Political Science, Jinan 250103, China
[3] School of Physics, Shandong University, Jinan 250100, China
* Correspondence: renjing19@sdjzu.edu.cn (J.R.); xiangjicai@foxmail.com (X.C.)

Abstract: We generalize an approach to studying the quantum state tomography (QST) of open systems in terms of the dynamical map in Kraus representation within the framework of dynamic generation of informationally complete positive operator-valued measures. As applications, we use the generalized approach to theoretically study the QST of qubit systems in the presence of nonequilibrium environments which exhibit nonstationary and non-Markovian random telegraph noise statistical properties. We derive the time-dependent measurement operators for the quantum state reconstruction of the single qubit and two-qubit systems in terms of the polarization operator basis. It is shown that the behavior of the time-dependent measurement operators is closely associated with the dynamical map of the qubit systems.

Keywords: quantum state tomography; decoherence; quantum measurement

1. Introduction

With the rapid development of quantum technologies, we can observe and control quantum systems and realize quantum information tasks at the scale of atoms and molecules in experiments. Quantum tomography is a fundamental approach that has been widely used to reconstruct the information of a physical system by analyzing the experimental measured data, which has potential applications in quantum state engineering, coherent manipulation and quantum control [1–3]. Three main types of quantum tomography are distinguished. Quantum process tomography can describe the evolution based on the dynamical map [4–7]. Quantum measurement tomography can obtain the characteristics of the actual operators governing the measurements [8–10]. Quantum state tomography (QST) can accurately reconstruct the representation of the state of the system based on the data measured from the experiments [11–21]. An important issue in QST is optimality, which refers to the maximization of the amount of information extracted from a single measurement. There are some standard approaches to realizing the optimality of QST: the maximum likelihood estimation (MLE) and the method of least squares [22,23], which have been widely used to study a variety of physical problems [24–26].

In most realistic situations, due to the inevitable influence of the environment, a quantum system is always regarded as open, and its quantum features gradually disappear during dynamical evolution. The study of quantum dynamics of open systems plays a fundamental role in quantum mechanical community and has drawn incrasing attention in physical research such as quantum computing, quantum metrology and quantum information science [27–47]. Quantum measurements of the dynamical properties of open quantum systems can help us to understand the environment's effects on the systems and the origins of the loss of coherence and quantum-classical transition in more depth [48–52]. Different from the closed systems with pure states under unitary evolution, the state of an open quantum system is generally mixed, and its dynamical evolution is no longer unified. By paying special attention to the proposals related to continuous measurements in the time domain, Czerwinski generalized the QST approach to the case of mixed quantum

Citation: Chen, H.; Han, T.; Chen, M.; Ren, J.; Cai, X.; Meng, X.; Peng, Y. Quantum State Tomography in Nonequilibrium Environments. *Photonics* **2023**, *10*, 134. https://doi.org/10.3390/photonics10020134

Received: 30 December 2022
Revised: 22 January 2023
Accepted: 26 January 2023
Published: 28 January 2023

states subject to random unitary maps within the framework of the dynamic generation of informationally complete, positive, operator-valued measures (IC-POVMs) (see, e.g., [53–56] and the review paper [57]).

In this paper, we further generalize the QST approach to the case of an open quantum system under non-unitary evolution, the state of which is governed by a dynamical map in the Kraus representation by means of IC-POVMs generated in the time domain. We use the generalized theory to study the QST of qubit systems in nonequilibrium environments, with the environmental noise exhibiting nonstationary random telegraph noise (RTN) statistical properties. We derive the time-dependent measurement operators in terms of the polarization operator basis of the single qubit and two-qubit systems, respectively. It is shown that the time-dependent measurement operators for the quantum state reconstruction are closely related to the dynamical map of the qubit systems.

This paper is organized as follows. In Section 2 we introduce the theoretical framework of QST in terms of the dynamic IC-POVMs generated by a dynamical map in the time domain. In Section 3, we study the QST of qubit systems coupled to nonequilibrium environments, which exhibit non-stationary and non-Markovian RTN statistical properties. In Section 4, we display the time-evolution of single qubit measurement operators using the trajectory representation on the Bloch sphere and discuss the environmental nonequilibrium effects on the time-dependent measurement operators. In Section 5, we provide the conclusions of the present study.

2. Theoretical Framework

QST in Terms of Dynamic Generation of IC-POVMs

QST aims to reconstruct the state of a quantum system described by, e.g., wave functions, state vectors and density matrices. In the following, we mainly focus on the state reconstruction in the density matrix representation. The state space $\mathcal{S}$ of a d-dimensional quantum system in density matrix representation consists of a set of Hermitian, positive and unit trace operators in Hilbert space $\mathcal{H}$ [58]

$$\mathcal{S} = \{\rho(t)\,|\,\rho(t) = \rho^{\dagger}(t), \rho(t) \geq 0, \mathrm{Tr}\rho(t) = 1\}. \tag{1}$$

Based on the postulates of quantum mechanics, quantum measurements are described by a set of measurement operators $\{M_j\}$ acting on the state space of the measured system, where the index n is associated with the experimental outcome of the measurement [59]. In accordance with Born's rule and by means of the Positive Operator-Valued Measure (POVM) formalism, for the initial quantum state $\rho(0)$ immediately before the measurement, the probability that outcome n occurs is written as

$$p_j(0) = \mathrm{Tr}[M_j\rho(0)], \tag{2}$$

where the probabilities $p_j(0)$ are sum up to one; namely, $\sum_j p_j(0) = 1$ and the POVM elements $0 \leq M_j \leq I_d$ satisfy the completeness condition $\sum_j M_j = I_d$ with I_d being the $d \times d$ identify operator. The set $\{M_j\}$ is referred to as a POVM related to the measurement. However, due to measurement errors, the experimental data associated with the expectations of the POVM elements may have negative eigenvalues, namely, nonphysical measured probabilities. A physical quantum state can be reconstructed from the negative measured probabilities using the MLE approach.

Appropriate measurements play a crucial role in QST because they can provide some information about an unknown quantum system. QST aims to estimate the state of the quantum system by analyzing the experimental measured data. Based on the outcome probabilities in Equation (2), we can obtain information about the quantum system immediately before measurement. To reconstruct any state, the set of operators $\{M_j\}$ must span the quantum state space $\mathcal{S}$, namely, the informational completeness. If the measurements are given in terms of IC-POVMs, we can obtain complete quantum information for the reconstruction of state $\rho(t)$. For a quantum state of dimension d, a single IC-POVM must provide d^2 linearly independent relations. Thus, an IC-POVM has at least d^2 elements of measurement and the minimal one has exactly d^2 operators. There might be an infinite number of sets of measurement operators to reconstruct a given quantum state within the QST framework. However, for some general cases, we may not have enough measurement operators to form an complete set for the tomographic reconstruction of the quantum state. In the following, we dynamically generalize the QST approach using an incomplete set of POVM in the time domain.

We consider an identically prepared quantum system evolving from an initial state $\rho(0)$ in terms of a dynamical map in the Kraus representation

$$\rho(t) = \Lambda(t)[\rho(0)] = \sum_{\mu} K_{\mu}(t)\rho(0)K_{\mu}^{\dagger}(t), \tag{3}$$

where $\Lambda(t)$ denotes a complete trace-preserving map and the Kraus operators satisfy the completeness condition $\sum_{\mu} K_{\mu}^{\dagger}(t)K_{\mu}(t) = I_d$. We also consider an incomplete set of POVM $\mathcal{M} = \{M_1, M_2, \cdots, M_r\}$ composed of r different operators, which can be measured at distinct time instants. By applying the dynamical map in Equation (3) to the measured results, we can obtain the time evolution of the probability related to the jth operator from the incomplete set $\mathcal{M}$

$$p_j(t) = \mathrm{Tr}[M_j\rho(t)] = \mathrm{Tr}\Big[M_j \sum_{\mu} K_{\mu}(t)\rho(0)K_{\mu}^{\dagger}(t)\Big] = \mathrm{Tr}[M_j(t)\rho(0)], \tag{4}$$

where $M_j(t) = \sum_{\mu} K_{\mu}^{\dagger}(t)M_jK_{\mu}(t)$ is the time-dependent operator. Due to the completeness condition $\sum_{\mu} K_{\mu}^{\dagger}(t)K_{\mu}(t) = I_d$ and the fact that $M_j \geq 0$, the time-dependent operator $M_n(t)$ is positive and semi-defined, which means that $M_j(t)$ satisfies the generalized measurement. Thus, if the number of the Kraus operators is k, we can select a discrete number of time instants $\{t_1, t_2, \cdots, t_k\}$ and obtain the time-dependent measured probabilities

$$\begin{aligned} p_j(t_1) &= \mathrm{Tr}[M_j(t_1)\rho(0)], \\ p_j(t_2) &= \mathrm{Tr}[M_j(t_2)\rho(0)], \\ &\vdots \\ p_j(t_k) &= \mathrm{Tr}[M_j(t_k)\rho(0)], \end{aligned} \tag{5}$$

which can be associated with the set of the time-dependent measurement operators $\mathcal{M}_t = \{M_1(t_1), \cdots, M_1(t_k), M_2(t_1), \cdots, M_2(t_k), \cdots, M_r(t_1), \cdots, M_r(t_k)\}$. In the context of state reconstruction, it is not necessary to consider a case with more measurement operators than k [56].

To realize the tomographic reconstruction of the initial state $\rho(0)$ in terms of the outcome and measured probabilities in Equations (2) and (5), the incomplete set $\mathcal{M}$, together with the time-dependent set $\mathcal{M}_t$ of the measurement operators, must satisfy the completeness condition

$$\sum_{j=1}^{r} M_j + \sum_{j=1}^{r}\sum_{l=1}^{k} M_j(t_l) = I_d. \tag{6}$$

That is, the union of sets $\mathcal{M}$ and $\mathcal{M}_t$ of the measurement operators forms an informationally complete set of POVM. Here, we have generalized the QST to the case governed by a dynamical map in the Kraus representation by means of IC-POVMs in the time domain. It is worth nothing that some elements of the union set of the measurement operators may be redundant. Generally, a standard IC-POVM for the reconstruction of a quantum state of dimension d has at least d^2 measurement operators. Thus, to realize QST of the information of the system, we can either choose enough measurement operators to form an IC-POVM that spans the entire Hilbert space of the quantum system or generalize an overcomplete set of measurement operators in the time domain, starting from an incomplete set of POVM less than d^2.

3. QST of Qubit Systems Coupled to Nonequilibrium Environments

Recently, much attention has been paid to studying the environmental nonequilibrium effects on quantum features, due to their significant role in the dynamical evolution of open quantum systems. In these processes, the environmental initial states, induced by the interaction with the quantum systems, cannot reach the stationary state in time [60–63], which corresponds to the idea that the environmental noise occurs in nonstationary statistics. The nonstationary and non-Markovian RTN has been widely used to study relevant issues regarding the dynamics of open quantum systems in nonequilibrium environments [64–71]. In the following, we theoretically studied the quantum state tomography of qubit systems in nonequilibrium environments exhibiting nonstationary and non-Markovian RTN statistical properties in terms of the generalized IC-POVMs.

3.1. QST of a Single Qubit System in Nonequilibrium Environments

As an application, we first considered the case of a single qubit system with the states $|1\rangle$ and $|0\rangle$, coupled to a nonequilibrium fluctuating environment. Within the framework of spectral diffusion established by Kubo and Anderson, the environmental influences give rise to the stochastic fluctuations in the frequency of single qubit system, of which the environmental noise is subject to a generalized RTN process exhibiting nonstationary and non-Markovian properties [64,65]. The open two-state system we considered could be chosen as a single-photon system consisting of the polarization states, e.g., horizontal $|H\rangle = |0\rangle$ and vertical $|V\rangle = |1\rangle$ and undergoes a pure decoherence process during dynamical evolution [65,72]

$$\frac{d}{dt}\rho_S(t) = i\frac{s(t)}{2}[\sigma_z, \rho_S(t)] + \frac{\gamma(t)}{2}[\sigma_z\rho_S(t)\sigma_z - \rho_S(t)], \tag{7}$$

where $\sigma_z = |H\rangle\langle H| - |V\rangle\langle V|$ denotes the Pauli matrix in the single-photon polarization basis $\mathscr{B}_S = \{|H\rangle, |V\rangle\}$, and the time-dependent frequency shift $s(t)$ and decoherence rate $\gamma(t)$ are, respectively, defined as

$$s(t) = -\mathrm{Im}\left[\frac{dF(t)/dt}{F(t)}\right], \gamma(t) = -\mathrm{Re}\left[\frac{dF(t)/dt}{F(t)}\right]. \tag{8}$$

Here, $F(t) = \left\langle \exp\left[i\int_0^t dt'\xi(t')\right]\right\rangle$ is the decoherence function, with $\langle\cdots\rangle$ being the average over the environmental noise $\xi(t)$ [65].

The pure decoherence only influences the coherence between the polarization components of the single-photon system. By taking an average of the environmental noise, the reduced density matrix of the single-photon system can be written in the Kraus operators representation as [71,73]

$$\rho_S(t) = \sum_{\mu=1}^{2} K_{S\mu}(t)\rho_S(0)K_{S\mu}^{\dagger}(t), \tag{9}$$

where the Kraus operators of the single-photon system satisfies

$$K_{S1}(t) = \begin{pmatrix} 1 & 0 \\ 0 & F(t) \end{pmatrix}, \quad K_{S2}(t) = \begin{pmatrix} 0 & 0 \\ 0 & \sqrt{1-|F(t)|^2} \end{pmatrix}. \tag{10}$$

The diagonal elements of the reduced density matrix of the single-photon system are time-independent $\rho_{HH}(t) = \rho_{HH}(0)$ and $\rho_{VV}(t) = 1 - \rho_{HH}(t)$, whereas the off-diagonal elements evolve over time

$$\rho_{HV}(t) = \rho^*_{VH}(t) = \rho_{HV}(0)F(t). \tag{11}$$

As in the standard RTN, the amplitude of the generalized RTN randomly jumps with the switching rate λ between the values $\pm\nu$. The environmental nonstationary property arises from the initial distribution $P(\xi_0, 0) = \frac{1}{2}(1-a)\delta_{\xi_0,-\nu} + \frac{1}{2}(1+a)\delta_{\xi_0,\nu}$ with the initial nonstationary parameter $-1 \leq a \leq 1$ [64,65]. The environmental non-Markovian property is described by a generalized master equation for the conditional probability related to an exponential memory kernel $K(t-t') = \kappa e^{-\kappa(t-t')}$ with the decay rate κ [74,75]. Correspondingly, the statistical characteristics associated with the first- and second-order moments of the environmental noise $\xi(t)$ can be expressed as

$$\langle \xi(t) \rangle = a\nu\mathcal{P}(t), \quad \langle \xi(t)\xi(t') \rangle = \nu^2\mathcal{P}(t-t'). \tag{12}$$

where $\mathcal{P}(t-t') = \mathscr{L}^{-1}[e^{-st'}\widetilde{\mathcal{P}}(s)]$ is the auxiliary probability function, with $\mathscr{L}^{-1}$ denoting the inverse Laplace transform and $\widetilde{\mathcal{P}}(s) = 1/[s + 2\lambda\widetilde{K}(s)]$. Based on the Bayes' theorem, the higher-order moments of the environmental noise can be factorized as products related to the second-order moments

$$\langle \xi(t_1)\xi(t_2)\cdots\xi(t_n) \rangle = \langle \xi(t_1)\xi(t_2) \rangle \langle \xi(t_3)\xi(t_4) \rangle \cdots \langle \xi(t_n) \rangle, \tag{13}$$

for the order of the time instants $t_1 > \cdots > t_n$ $(n \geq 3)$.

According to the statistical characteristics of the environmental noise, and in terms of the Dyson expansion for the decoherence function, we can obtain a closed third-order differential equation for the decoherence function [64]

$$\frac{d^3}{dt^3}F(t) + \kappa\frac{d^2}{dt^2}F(t) + (2\kappa\lambda + \nu^2)\frac{d}{dt}F(t) + \kappa\nu^2F(t) = 0, \tag{14}$$

with the initial conditions $F(0) = 1$, $(d/dt)F(0) = ia\nu$ and $(d^2/dt^2)F(0) = -\nu^2$. Correspondingly, the decoherence function $F(t)$ for the single qubit system can be exactly expressed as

$$F(t) = \mathscr{L}^{-1}[\mathcal{F}(p)], \quad \mathcal{F}(p) = \frac{p^2 + \kappa p + 2\kappa\lambda + ia\nu(p+\kappa)}{p^3 + \kappa p^2 + (2\kappa\lambda + \nu^2)p + \kappa\nu^2}. \tag{15}$$

As the statistical properties of the generalized RTN extracted from the standard RTN are non-Markovian, nonstationary and time-homogeneous, the environmental nonequilibrium effects arising from the nonstationary parameter are only associated with the odd-order moments of the environmental noise [64,65]. Thus, this only influences the imaginary component of the decoherence function, as in Equation (15). It has been shown that the nonequilibrium effects of the environment can suppress decoherence of the quantum system and decrease non-Markovianity in the dynamical evolution of a single qubit system [64,65].

In terms of the computational basis $\mathscr{P} = \{|H\rangle, |V\rangle, |D\rangle, |A\rangle, |L\rangle, |R\rangle\}$, a typical POVM can be expressed with six polarization states: horizontal $|H\rangle = |0\rangle$, vertical $|V\rangle = |1\rangle$, diagonal $|D\rangle = (|H\rangle + V\rangle)/\sqrt{2}$, antidiagonal $|A\rangle = (|H\rangle - |V\rangle)/\sqrt{2}$, left-circular $|L\rangle = (|H\rangle - i|V\rangle)/\sqrt{2}$ and right-circular $|R\rangle = (|H\rangle + i|V\rangle)/\sqrt{2}$ [12,56,76]. The six polarization states can be divided into three elements of a set of orthogonal bases associated with mutually unbiased bases in a two-dimensional Hilbert space (see Appendix A). Based on the set of orthogonal bases, we can obtain an overcomplete set of measurement operators. From the Born rule for the probability of the single-photon system

$$p^S(t) = \mathrm{Tr}[M^S \rho_S(t)] = \mathrm{Tr}\Big[M^S \sum_\mu K_{S\mu}(t)\rho_S(0)K^\dagger_{S\mu}(t)\Big] = \mathrm{Tr}[M^S(t)\rho_S(0)], \tag{16}$$

we can obtain the time-dependent measurement operator of the single-photon system $M^S(t) = \sum_\mu K^\dagger_{S\mu}(t)M^S K_{S\mu}(t)$. For the given measurement operator $M^S_j = |j\rangle\langle j|(j = H, V, D, A, L, R)$, we can obtain the time-dependent operator of measurement

$$M^S_j(t) = \sum_{\mu=1}^{2} K^\dagger_{S\mu}(t)M^S_j K_{S\mu}(t) = \begin{pmatrix} M^{11}_j & M^{12}_j F(t) \\ M^{21}_j F^*(t) & M^{22}_j \end{pmatrix}. \tag{17}$$

The time-evolution of the measurement operator $M^S_j(t)$ of the single-photon system closely depends on the decoherence effect quantified by the decoherence function $F(t)$, and the initial measurement operator M^S_j. Equation (17) correspond to six time-dependent measurement operators with the following expressions:

$$\begin{aligned}
M^S_H(t) &= \sum_{\mu=1}^{2} K^\dagger_{S\mu}(t)M^S_H K_{S\mu}(t) = M^S_H = \begin{pmatrix} 1 & 0 \\ 0 & 0 \end{pmatrix}, \\
M^S_V(t) &= \sum_{\mu=1}^{2} K^\dagger_{S\mu}(t)M^S_V K_{S\mu}(t) = M^S_V = \begin{pmatrix} 0 & 0 \\ 0 & 1 \end{pmatrix}, \\
M^S_D(t) &= \sum_{\mu=1}^{2} K^\dagger_{S\mu}(t)M^S_D K_{S\mu}(t) = \frac{1}{2}\begin{pmatrix} 1 & F(t) \\ F^*(t) & 1 \end{pmatrix}, \\
M^S_A(t) &= \sum_{\mu=1}^{2} K^\dagger_{S\mu}(t)M^S_A K_{S\mu}(t) = \frac{1}{2}\begin{pmatrix} 1 & -F(t) \\ -F^*(t) & 1 \end{pmatrix}, \\
M^S_L(t) &= \sum_{\mu=1}^{2} K^\dagger_{S\mu}(t)M^S_L K_{S\mu}(t) = \frac{1}{2}\begin{pmatrix} 1 & iF(t) \\ -iF^*(t) & 1 \end{pmatrix}, \\
M^S_R(t) &= \sum_{\mu=1}^{2} K^\dagger_{S\mu}(t)M^S_R K_{S\mu}(t) = \frac{1}{2}\begin{pmatrix} 1 & -iF(t) \\ iF^*(t) & 1 \end{pmatrix}.
\end{aligned} \tag{18}$$

The two measurement operators $M^S_H(t)$ and $M^S_V(t)$ do not evolve over time, whereas the other four measurement operators $M^S_D(t)$, $M^S_A(t)$, $M^S_L(t)$ and $M^S_R(t)$ are closely associated with the decoherence function $F(t)$.

3.2. QST of a Two-Qubit System in Nonequilibrium Environments

As another application, we can consider the case of a two-qubit system T consisting of two noninteracting identical single qubits A and B, which are independently coupled to its local nonequilibrium environment, respectively. The initial state of the system can be written as a product state between the two single qubits. This physical model can be considered as a two-photon system, of which each photon interacts with its pure decoherence environment and loses coherence between its polarization components.

As there are no initial interactions between the two single qubits A and B, the dynamics of the two-photon system can be constructed from that of a single-photon system in the Kraus operators' representation [77,78]. By taking an average of the environmental noise, the reduced density matrix of the two-photon system can be expressed, in terms of the standard product basis $\mathscr{B}_T = \{|1\rangle = |HH\rangle, |2\rangle = |HV\rangle, |3\rangle = |VH\rangle, |4\rangle = |VV\rangle\}$ in the Kraus operators representation, as [71]

$$\rho_T(t) = \sum_{\mu=1}^{4} K_{T\mu}(t)\rho_T(0)K_{T\mu}^{\dagger}(t), \tag{19}$$

where the two-photon Kraus operators $K_{T\mu}(t) = K_{S\nu}(t) \otimes K_{S\upsilon}(t)$ $(\nu, \upsilon = 1, 2)$ are the tensor products of the single-photon Kraus operators

$$\begin{aligned}
K_{T1}(t) &= \begin{pmatrix} 1 & 0 \\ 0 & F(t) \end{pmatrix} \otimes \begin{pmatrix} 1 & 0 \\ 0 & F(t) \end{pmatrix}, \\
K_{T2}(t) &= \begin{pmatrix} 1 & 0 \\ 0 & F(t) \end{pmatrix} \otimes \begin{pmatrix} 1 & 0 \\ 0 & \sqrt{1-|F(t)|^2} \end{pmatrix}, \\
K_{T3}(t) &= \begin{pmatrix} 0 & 0 \\ 0 & \sqrt{1-|F(t)|^2} \end{pmatrix} \otimes \begin{pmatrix} 1 & 0 \\ 0 & F(t) \end{pmatrix}, \\
K_{T4}(t) &= \begin{pmatrix} 0 & 0 \\ 0 & \sqrt{1-|F(t)|^2} \end{pmatrix} \otimes \begin{pmatrix} 0 & 0 \\ 0 & \sqrt{1-|F(t)|^2} \end{pmatrix}.
\end{aligned} \tag{20}$$

Correspondingly, the diagonal elements do not evolve over time $\rho_{11}(t) = \rho_{11}(0)$, $\rho_{22}(t) = \rho_{22}(0)$, $\rho_{33}(t) = \rho_{33}(0)$ and $\rho_{44}(t) = 1 - [\rho_{11}(0) + \rho_{22}(0) + \rho_{33}(0)]$ whereas the off-diagonal elements are time-dependent

$$\begin{aligned}
\rho_{21}(t) &= \rho_{12}^*(t) = \rho_{21}(0)F(t), \\
\rho_{31}(t) &= \rho_{13}^*(t) = \rho_{31}(0)F(t), \\
\rho_{32}(t) &= \rho_{23}^*(t) = \rho_{32}(0)|F(t)|^2, \\
\rho_{41}(t) &= \rho_{14}^*(t) = \rho_{41}(0)F^2(t), \\
\rho_{42}(t) &= \rho_{24}^*(t) = \rho_{42}(0)F(t), \\
\rho_{43}(t) &= \rho_{34}^*(t) = \rho_{43}(0)F(t).
\end{aligned} \tag{21}$$

Based on the Born rule for the probability of the two-photon system

$$p^T(t) = \mathrm{Tr}[M^T\rho_T(t)] = \mathrm{Tr}\Big[M^T\sum_{\mu} K_{T\mu}(t)\rho_T(0)K_{T\mu}^{\dagger}(t)\Big] = \mathrm{Tr}[M^T(t)\rho_T(0)], \tag{22}$$

we can obtain the time-dependent measurement operator of the two-photon system $M^T(t) = \sum_{\mu} K_{T\mu}^{\dagger}(t)M^T K_{T\mu}(t)$. In terms of the six polarization bases for the single-photon system $\mathscr{P} = \{|H\rangle, |V\rangle, |D\rangle, |A\rangle, |L\rangle, |R\rangle\}$, we can obtain an overcomplete set of 36 time-dependent measurement operators for the two-photon system

$$M_{kl}^T(t) = \sum_{\mu=1}^{4} K_{T\mu}^{\dagger}(t)M_{kl}^T K_{T\mu}(t) = \sum_{\mu=1}^{2} K_{S\mu}^{\dagger}(t)M_k^S K_{S\mu}(t) \otimes \sum_{\mu=1}^{2} K_{S\mu}^{\dagger}(t)M_l^S K_{S\mu}(t), \tag{23}$$

where $M_{kl}^T = M_k^S \otimes M_l^S = |k\rangle\langle k| \otimes |l\rangle\langle l| (k, l = H, V, D, A, L, R)$ denote the initial measurement operators of the two-photon system. The two-qubit measurement operators are the tensor products of single-photon ones due to the fact that the two single-photon systems are independent of each other. In the matrix representation, the time-dependent measurement operator in Equation (23) can be expressed as

$$M_{kl}^T(t) = \begin{pmatrix} M_{kl}^{11} & M_{kl}^{12}F(t) & M_{kl}^{13}F(t) & M_{kl}^{14}F^2(t) \\ M_{kl}^{21}F^*(t) & M_{kl}^{22} & M_{kl}^{23}|F(t)|^2 & M_{kl}^{24}F(t) \\ M_{kl}^{31}F^*(t) & M_{kl}^{32}|F(t)|^2 & M_{kl}^{33} & M_{kl}^{34}F(t) \\ M_{kl}^{41}F^{*2}(t) & M_{kl}^{42}F^*(t) & M_{kl}^{43}F^*(t) & M_{kl}^{44} \end{pmatrix}. \tag{24}$$

Similarly to the case of a single qubit, the measurement operators for the two-qubit system in Equation (24) are also closely related to the decoherence function $F(t)$ and the initial measurement operators M^T_{kl}. Based on Equation (24), some typical time-dependent measurement operators can be expressed as

$$
\begin{aligned}
M^T_{HH}(t) &= \begin{pmatrix} 1 & 0 & 0 & 0 \\ 0 & 0 & 0 & 0 \\ 0 & 0 & 0 & 0 \\ 0 & 0 & 0 & 0 \end{pmatrix}, \\
M^T_{HD}(t) &= \frac{1}{2}\begin{pmatrix} 1 & F(t) & 0 & 0 \\ F^*(t) & 1 & 0 & 0 \\ 0 & 0 & 0 & 0 \\ 0 & 0 & 0 & 0 \end{pmatrix}, \\
M^T_{HR}(t) &= \frac{1}{2}\begin{pmatrix} 1 & -iF(t) & 0 & 0 \\ iF^*(t) & 1 & 0 & 0 \\ 0 & 0 & 0 & 0 \\ 0 & 0 & 0 & 0 \end{pmatrix}, \\
M^T_{DD}(t) &= \frac{1}{4}\begin{pmatrix} 1 & F(t) & F(t) & F^2(t) \\ F^*(t) & 1 & |F(t)|^2 & F(t) \\ F^*(t) & |F(t)|^2 & 1 & F(t) \\ F^{*2}(t) & F^*(t) & F^*(t) & 1 \end{pmatrix}, \\
M^T_{DR}(t) &= \frac{1}{4}\begin{pmatrix} 1 & -iF(t) & F(t) & -iF^2(t) \\ iF^*(t) & 1 & i|F(t)|^2 & F(t) \\ F^*(t) & -i|F(t)|^2 & 1 & -iF(t) \\ iF^{*2}(t) & F^*(t) & iF^*(t) & 1 \end{pmatrix}, \\
M^T_{RR}(t) &= \frac{1}{4}\begin{pmatrix} 1 & -iF(t) & -iF(t) & -F^2(t) \\ iF^*(t) & 1 & |F(t)|^2 & -iF(t) \\ iF^*(t) & |F(t)|^2 & 1 & -iF(t) \\ -F^{*2}(t) & iF^*(t) & iF^*(t) & 1 \end{pmatrix}.
\end{aligned}
\tag{25}
$$

In addition to the QST of a two-photon physical system, some useful physical quantities of the system, such as the concurrence, the negativity, the classical and quantum correlations, can be also obtained based on the corresponding formulas from the reconstructed quantum state [20].

4. Results and Discussion

In this section, we show the results of the QST of qubit systems coupled to nonequilibrium environments and study the nonequilibrium effects of the environments on the state reconstruction. To intuitively display the behavior of the time evolution of the measurement operators $M^S_D(t)$, $M^S_A(t)$, $M^S_L(t)$ and $M^S_R(t)$, we plot the trajectories of them on the Bloch sphere by expressing $M^S(t) = 1/2[I_2 + \sum_{j=x,y,z} r_j(t)\sigma_j]$ with $r_j(t) = \mathrm{Tr}[M^S(t)\sigma_j]$. The decoherence rate $\gamma(t)$ and frequency shift $s(t)$ describe the normal and tangential slopes of the radius $r(t) = \sqrt{\sum_{j=x,y,z} r^2_j(t)}$, respectively, and the rate of change of the radius $r(t)$ is related to the non-Markovian feature of the dynamical evolution.

As shown in Figure 1, the time evolution of the measurement operators $M^S_D(t)$, $M^S_A(t)$, $M^S_L(t)$ and $M^S_R(t)$ displays monotonic behavior in Markovian dynamics regime, whereas it shows non-monotonic behavior in the non-Markovian dynamics regime. This results from the time-dependent measurement operators generated from the dynamical map of the single-qubit system in terms of the Kraus operators in Equation (10). In addition, the initial coordinates (r_x, r_y, r_z) for the measurement operators and the directions of rotation in non-Markovian dynamics regime are different, as, to effectively reconstruct a quantum state, the measurement operators must satisfy the completeness condition. Furthermore, the radii for the measurement operators reduce to zero in the long time limit. This is due to the fact that the decoherence effect induced by the environmental noise results in the vanishing of the off-diagonal elements of the reduced density matrix of the single-qubit system in the long time limit.

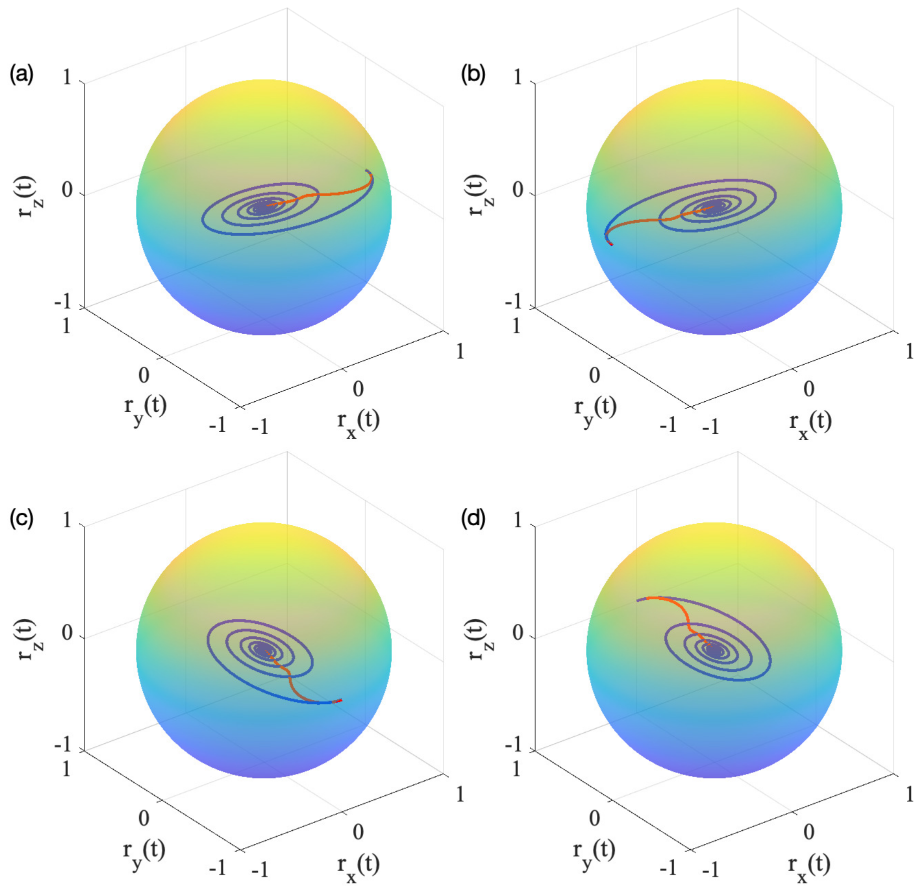

Figure 1. (Color online) Trajectories of the measurement operators (**a**) $M_D^S(t)$, (**b**) $M_A^S(t)$, (**c**) $M_L^S(t)$ and (**d**) $M_R^S(t)$ on the Bloch sphere. The red lines stand for the Markovian dynamics regime with $\nu/\lambda = 0.8$ and $\kappa/\lambda = 2$ and the blue lines represent the non-Markovian dynamics regime with $\nu/\lambda = 3$ and $\kappa/\lambda = 2$. The initial nonstationary parameter is chosen as $a = 0.5$.

As the behavior of the time evolution of the measurement operators $M_D^S(t)$, $M_A^S(t)$, $M_L^S(t)$ and $M_R^S(t)$ is similar, to further display how the environmental nonequilibrium effects influence the time-evolution of the measurement operators, we plot the measurement operator $M_A^S(t)$ as a simple example in the trajectory representation on the Bloch sphere for the different values of the initial nonstationary parameter a.

As displayed in Figure 2, the trajectories of the measurement operator $M_A^S(t)$ display monotonic behavior in Markovian dynamics regime, whereas non-monotonic behavior is shown in the non-Markovian dynamics regime. In addition, as the environment moves away from equilibrium (the absolute value of the initial nonstationary parameter a departs from zero), the radius $r(t)$ of the measurement operator on the Bloch sphere in the trajectory representation becomes longer in both the Markovian and non-Markovian dynamics regimes. This is because the environmental nonequilibrium effects can reduce the dynamical decoherence of the system and can enhance the frequency shift $s(t)$ in the dynamical evolution of the system. Furthermore, the trajectory of the measurement operator $M_A^S(t)$ shows the symmetry for the initial nonstationary parameter a, taking positive and negative values in both the Markovian and non-Markovian dynamics regimes. This is because the direction of rotation of the measurement operator $M_A^S(t)$ in the trajectory representation is closely associated with the symmetrical behavior in the time evolution of the frequency shift $s(t)$ for positive and negative values of the initial nonstationary parameter a.

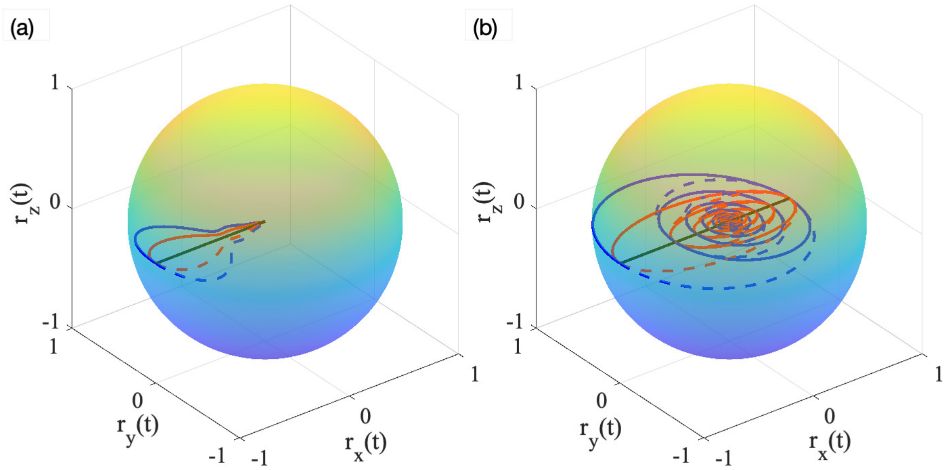

Figure 2. (Color online) Trajectories of the measurement operator $M_A^S(t)$ on the Bloch sphere for for different values of the initial nonstationary parameter a in (**a**) Markovian dynamics regime with $\nu/\lambda = 0.8$ and $\kappa/\lambda = 2$ and (**b**) non-Markovian dynamics regime with $\nu/\lambda = 3$ and $\kappa/\lambda = 2$. Blue lines for $a = \pm 1$; red lines for $a = \pm 0.5$ and black lines for $a = 0$ (the solid and dashed lines represent positive and negative values of a, respectively.)

5. Conclusions

QST aims to reconstruct the state of a quantum system by analyzing the experimental measured data with appropriate measurements. In this paper, we generalized the QST approach to a non-unitary evolution of open quantum systems in terms of a dynamical map, using IC-POVMs generated in the time domain. The generalized QST can reconstruct a d-dimensional quantum state from an incomplete set of measurement operators less than d^2, which is more efficient than the standard QST approach. As applications, we used the generalized QST approach to study the QST of qubit systems in nonequilibrium environments, with the environmental noise exhibiting nonstationary and non-Markovian RTN statistical properties. In terms of the polarization operator basis, we derived the time-dependent measurement operators related to the reconstruction of the states of the single-qubit and two-qubit systems, respectively. The behavior of the trajectories of the time-dependent measurement operators on the Bloch sphere is closely associated with the dynamic regimes of the quantum systems. Our results are significant to quantum information processing and helpful in the further understanding of the QST of open quantum systems.

Author Contributions: Conceptualization, J.R., X.C., X.M. and Y.P.; Formal analysis, H.C., T.H., M.C. and X.C.; Writing—original draft preparation, H.C. and X.C.; Writing—review and editing, J.R., X.C., X.M. and Y.P. All authors have read and agreed to the published version of the manuscript.

Acknowledgments: We sincerely acknowledge Prof. Artur Czerwinski for his valuable suggestions and useful discussions on this study.

Funding: This work was supported by the National Natural Science Foundation of China (Grant No. 12005121), the Natural Science Foundation of Shandong Province (Grant No. ZR2021LLZ009), the Youth Innovation Science and Technology Support Program of Universities in Shandong Province (Grant No. 2021KJ082) and the Doctoral Research Fund of Shandong Jianzhu University (Grant No. X19040Z).

Institutional Review Board Statement: Not applicable.

Informed Consent Statement: Not applicable.

Data Availability Statement: Not applicable.

Conflicts of Interest: The authors declare no conflict of interest.

Abbreviations

The following abbreviations are used in this manuscript:

QST	quantum state tomography
MLE	maximum likelihood estimation
POVM	positive operator-valued measure
RTN	random telegraph noise

Appendix A. State Representations of a *d*-Dimensional Quantum System

The quantum state $\rho_d(t)$ for a system of dimension d (a qudit system) can generally be expressed in the coherent state representation in terms of the generalized Gell–Mann matrix basis as [12,79,80]

$$\rho_d(t) = \frac{1}{d}\left[I_d + \sum_{j=1}^{d^2-1} r_j(t)\sigma_j\right], \tag{A1}$$

where σ_j are Hermitian, traceless and orthogonal generators of algebra $\mathrm{SU}(d)$ and $r_j(t) = \mathrm{Tr}[\rho_d(t)\sigma_j]$ are the Bloch vectors. A systematic construction of the generators of algebra $\mathrm{SU}(d)$ with $d(d-1)$ off-diagonal and $(d-1)$ diagonal elements can be expressed as

$$\{\sigma_j\}_{j=1}^{d^2-1} = \{\Lambda_{kl}^s, \Lambda_{kl}^a, \Lambda_m\}. \tag{A2}$$

The $d(d-1)/2$ symmetric, $d(d-1)/2$ antisymmetric and diagonal components are, respectively, given by

$$\begin{aligned} &\Lambda_{kl}^s = e_{k,l} + e_{l,k}, \quad \Lambda_{kl}^a = -i(e_{k,l} - e_{l,k}), \\ &\Lambda_m = \sqrt{\frac{2}{m(m+1)}} \sum_{j=1}^{m} \Big(e_{j,j} - m e_{(m+1),(m+1)}\Big), \end{aligned} \tag{A3}$$

where $e_{k,l} = |k\rangle\langle l|$ and $e_{l,k} = |l\rangle\langle k|$ are the elementary raising and lowering operators with $1 \leq k < l \leq d$, and $e_{m,m} = |m\rangle\langle m|$ are the elementary diagonal operators with $1 \leq m \leq d-1$. As generators of algebra $\mathrm{SU}(d)$ are all traceless, their linear combination does not correspond to any quantum state. Thus, to define a physical state, we must combine these generators σ_j with the identify matrix I_d. For a quantum system composed of n qudit systems, the generalized coherent state representation for the state $\rho_{nd}(t)$ of dimension d^n can be written as

$$\rho_{nd}(t) = \frac{1}{d^n}\left[I_d \otimes \cdots \otimes I_d + \sum_{j_1,\cdots,j_n=1}^{d^2-1} r_{j_1}(t)\cdots r_{j_n}(t)\sigma_{j_1} \otimes \cdots \otimes \sigma_{j_n}\right], \tag{A4}$$

where $r_{j_1}(t)\cdots r_{j_n}(t) = \mathrm{Tr}[\rho_{nd}(t)\sigma_{j_1} \otimes \cdots \otimes \sigma_{j_n}]$ which span the space of operators by the n tensor product of the generators $\mathrm{SU}(d) \otimes \cdots \otimes \mathrm{SU}(d)$.

The density matrix $\rho_d(t)$ of a d-dimensional qudit system can also be decomposed in terms of the widely used polarization operator basis as [80]

$$\rho_d(t) = \frac{1}{d}\left[I_d + \sum_{l=1}^{2s}\sum_{m=-l}^{l} R_{lm}(t)\Sigma_{lm}\right], \tag{A5}$$

where $\Sigma_{lm} = \sqrt{(2l+1)/(2s+1)}\sum_{k,l=1}^{d} C_{s,m_l,lm}^{s,m_k} e_{k,l}$ are the polarization operators in the Hilbert–Schmidt space with $C_{s,m_l,lm}^{s,m_k}$ being the Clebsch–Gordan coefficients and the indices satisfying $s = (d-1)/2$, $l = 0, 1, \cdots, 2s$, $m = -l, -l+1, \cdots, l-1, l$ and $m_1 = s, m_2 = s-1, \cdots, m_d = -s$, and $R_{lm}(t) = \mathrm{Tr}[\Sigma_{lm}^{\dagger}\rho_d(t)]$ are the components of decomposition. The polarization operators (except $\Sigma_{00} = \sqrt{1/d}\,I_d$) are traceless and non-Hermitian; thus, the components $R_{lm}(t)$ are generally complex. Correspondingly, the quantum state of a n-qudit system can be expanded in terms of the polarization operator basis as follows:

$$\rho_{nd}(t) = \frac{1}{d^n}\left[I_d \otimes \cdots \otimes I_d + \sum_{l_1,\cdots,l_n=1}^{2s} \sum_{\substack{m_1=-l_1,\\ \cdots,\\ m_n=-l_n}}^{l_1,\cdots,l_n} R_{l_1 m_1}(t)\cdots R_{l_n m_n}(t)\Sigma_{l_1 m_l} \otimes \cdots \otimes \Sigma_{l_n m_n} \right], \tag{A6}$$

where $R_{l_1 m_1}(t)\cdots R_{l_n m_n}(t) = \mathrm{Tr}[\Sigma^\dagger_{l_1 m_l} \otimes \cdots \otimes \Sigma^\dagger_{l_n m_n}\rho_{nd}(t)]$ are the components of polarization decomposition of the n-qudit system.

References

1. Sedziak-Kacprowicz, K.; Czerwinski, A.; Kolenderski, P. Tomography of time-bin quantum states using time-resolved detection. *Phys. Rev. A* **2020**, *102*, 052420. https://doi.org/10.1103/PhysRevA.102.052420.
2. Czerwinski, A.; Sedziak-Kacprowicz, K.; Kolenderski, P. Phase estimation of time-bin qudits by time-resolved single-photon counting. *Phys. Rev. A* **2021**, *103*, 042402. https://doi.org/10.1103/PhysRevA.103.042402.
3. Czerwinski, A. Hamiltonian tomography by the quantum quench protocol with random noise. *Phys. Rev. A* **2021**, *104*, 052431. https://doi.org/10.1103/PhysRevA.104.052431.
4. Altepeter, J.B.; Branning, D.; Jeffrey, E.; Wei, T.C.; Kwiat, P.G.; Thew, R.T.; O'Brien, J.L.; Nielsen, M.A.; White, A.G. Ancilla-Assisted Quantum Process Tomography. *Phys. Rev. Lett.* **2003**, *90*, 193601. https://doi.org/10.1103/PhysRevLett.90.193601.
5. O'Brien, J.L.; Pryde, G.J.; Gilchrist, A.; James, D.F.V.; Langford, N.K.; Ralph, T.C.; White, A.G. Quantum Process Tomography of a Controlled-NOT Gate. *Phys. Rev. Lett.* **2004**, *93*, 080502. https://doi.org/10.1103/PhysRevLett.93.080502.
6. Mohseni, M.; Rezakhani, A.T.; Lidar, D.A. Quantum-process tomography: Resource analysis of different strategies. *Phys. Rev. A* **2008**, *77*, 032322. https://doi.org/10.1103/PhysRevA.77.032322.
7. White, G.; Pollock, F.; Hollenberg, L.; Modi, K.; Hill, C. Non-Markovian Quantum Process Tomography. *PRX Quantum* **2022**, *3*, 020344. https://doi.org/10.1103/PRXQuantum.3.020344.
8. Luis, A.; Sánchez-Soto, L.L. Complete Characterization of Arbitrary Quantum Measurement Processes. *Phys. Rev. Lett.* **1999**, *83*, 3573–3576. https://doi.org/10.1103/PhysRevLett.83.3573.
9. Lundeen, J.S.; Feito, A.; Coldenstrodt-Ronge, H.; Pregnell, K.L.; Silberhorn, C.; Ralph, T.C.; Eisert, J.; Plenio, M.B.; Walmsley, I.A. Tomography of quantum detectors. *Nat. Phys.* **2009**, *5*, 27. https://doi.org/10.1038/nphys1133.
10. Cónsul, R.; Luis, A. Detector self-tomography. *Opt. Lett.* **2020**, *45*, 6799. https://doi.org/10.1364/OL.410265.
11. James, D.F.V.; Kwiat, P.G.; Munro, W.J.; White, A.G. Measurement of qubits. *Phys. Rev. A* **2001**, *64*, 052312. https://doi.org/10.1103/PhysRevA.64.052312.
12. Thew, R.T.; Nemoto, K.; White, A.G.; Munro, W.J. Qudit quantum-state tomography. *Phys. Rev. A* **2002**, *66*, 012303. https://doi.org/10.1103/PhysRevA.66.012303.
13. Czerwinski, A. Quantum tomography of entangled qubits by time-resolved single-photon counting with time-continuous measurements. *Quantum Inf. Process.* **2021**, *21*, 332. https://doi.org/10.1007/s11128-022-03682-8.
14. Christandl, M.; Renner, R. Reliable Quantum State Tomography. *Phys. Rev. Lett.* **2012**, *109*, 120403. https://doi.org/10.1103/PhysRevLett.109.120403.
15. Xin, T.; Lu, D.; Klassen, J.; Yu, N.; Ji, Z.; Chen, J.; Ma, X.; Long, G.; Zeng, B.; Laflamme, R. Quantum State Tomography via Reduced Density Matrices. *Phys. Rev. Lett.* **2017**, *118*, 020401. https://doi.org/10.1103/PhysRevLett.118.020401.
16. Bent, N.; Qassim, H.; Tahir, A.A.; Sych, D.; Leuchs, G.; Sánchez-Soto, L.L.; Karimi, E.; Boyd, R.W. Experimental Realization of Quantum Tomography of Photonic Qudits via Symmetric Informationally Complete Positive Operator-Valued Measures. *Phys. Rev. X* **2015**, *5*, 041006. https://doi.org/10.1103/PhysRevX.5.041006.
17. Gupta, R.; Xia, R.; Levine, R.D.; Kais, S. Maximal Entropy Approach for Quantum State Tomography. *PRX Quantum* **2021**, *2*, 010318. https://doi.org/10.1103/PRXQuantum.2.010318.
18. Stricker, R.; Meth, M.; Postler, L.; Edmunds, C.; Ferrie, C.; Blatt, R.; Schindler, P.; Monz, T.; Kueng, R.; Ringbauer, M. Experimental Single-Setting Quantum State Tomography. *PRX Quantum* **2022**, *3*, 040310. https://doi.org/10.1103/PRXQuantum.3.040310.
19. Czerwinski, A. Optimal evolution models for quantum tomography. *J. Phys. A* **2016**, *49*, 075301. https://doi.org/10.1088/1751-8113/49/7/075301.
20. Czerwinski, A.; Szlachetka, J. Efficiency of photonic state tomography affected by fiber attenuation. *Phys. Rev. A* **2022**, *105*, 062437. https://doi.org/10.1103/PhysRevA.105.062437.
21. Czerwinski, A.; Czerwinska, K. Statistical Analysis of the Photon Loss in Fiber-Optic Communication. *Photonics* **2022**, *9*, 568. https://doi.org/10.3390/photonics9080568.
22. Hradil, Z. Quantum-state estimation. *Phys. Rev. A* **1997**, *55*, R1561. https://doi.org/10.1103/PhysRevA.55.R1561.
23. Opatrný, T.; Welsch, D.G.; Vogel, W. Least-squares inversion for density-matrix reconstruction. *Phys. Rev. A* **1997**, *56*, 1788. https://doi.org/10.1103/PhysRevA.56.1788.
24. Banaszek, K.; D'Ariano, G.M.; Paris, M.G.A.; Sacchi, M.F. Maximum-likelihood estimation of the density matrix. *Phys. Rev. A* **1999**, *61*, 010304. https://doi.org/10.1103/PhysRevA.61.010304.

25. Smolin, J.A.; Gambetta, J.M.; Smith, G. Efficient Method for Computing the Maximum-Likelihood Quantum State from Measurements with Additive Gaussian Noise. *Phys. Rev. Lett.* **2012**, *108*, 070502. https://doi.org/10.1103/PhysRevLett.108.070502.
26. Shang, J.; Zhang, Z.; Ng, H.K. Superfast maximum-likelihood reconstruction for quantum tomography. *Phys. Rev. A* **2017**, *95*, 062336. https://doi.org/10.1103/PhysRevA.95.062336.
27. Breuer, H.P.; Petruccione, F. *The Theory of Open Quantum Systems*; Oxford University Press: New York, NY, USA, 2002.
28. Schlosshauer, M. *Decoherence and the Quantum-to-Classical Transition*; Springer: Berlin/Heidelberg, Germnay, 2007.
29. Schlosshauer, M. Quantum decoherence. *Phys. Rep.* **2019**, *831*, 1. https://doi.org/10.1016/j.physrep.2019.10.001.
30. Carollo, A.; Valenti, D.; Spagnolo, B. Geometry of quantum phase transitions. *Phys. Rep.* **2020**, *838*, 1. https://doi.org/10.1016/j.physrep.2019.11.002.
31. Piilo, J.; Maniscalco, S.; Härkönen, K.; Suominen, K.A. Non-Markovian Quantum Jumps. *Phys. Rev. Lett.* **2008**, *100*, 180402. https://doi.org/10.1103/PhysRevLett.100.180402.
32. Breuer, H.; Laine, E.; Piilo, J. Measure for the Degree of Non-Markovian Behavior of Quantum Processes in Open Systems. *Phys. Rev. Lett.* **2009**, *103*, 210401. https://doi.org/10.1103/PhysRevLett.103.210401.
33. Rivas, A.; Huelga, S.F.; Plenio, M.B. Entanglement and Non-Markovianity of Quantum Evolutions. *Phys. Rev. Lett.* **2010**, *105*, 050403. https://doi.org/10.1103/PhysRevLett.105.050403.
34. Zhang, W.M.; Lo, P.Y.; Xiong, H.N.; Tu, M.W.Y.; Nori, F. General Non-Markovian Dynamics of Open Quantum Systems. *Phys. Rev. Lett.* **2012**, *109*, 170402. https://doi.org/10.1103/PhysRevLett.109.170402.
35. Chruściński, D.; Maniscalco, S. Degree of Non-Markovianity of Quantum Evolution. *Phys. Rev. Lett.* **2014**, *112*, 120404. https://doi.org/10.1103/PhysRevLett.112.120404.
36. Rivas, A.; Huelga, S.F.; Plenio, M.B. Quantum non-Markovianity: characterization, quantification and detection. *Rep. Prog. Phys.* **2014**, *77*, 094001. https://doi.org/10.1088/0034-4885/77/9/094001.
37. Fanchini, F.F.; Karpat, G.; Çakmak, B.; Castelano, L.K.; Aguilar, G.H.; Farías, O.J.; Walborn, S.P.; Ribeiro, P.H.S.; de Oliveira, M.C. Non-Markovianity through Accessible Information. *Phys. Rev. Lett.* **2014**, *112*, 210402. https://doi.org/10.1103/PhysRevLett.112.210402.
38. Breuer, H.; Laine, E.; Piilo, J.; Vacchini, B. *Colloquium*: Non-Markovian dynamics in open quantum systems. *Rev. Mod. Phys.* **2016**, *88*, 021002. https://doi.org/10.1103/RevModPhys.88.021002.
39. de Vega, I.; Alonso, D. Dynamics of non-Markovian open quantum systems. *Rev. Mod. Phys.* **2017**, *89*, 015001. https://doi.org/10.1103/RevModPhys.89.015001.
40. Sun, S.; Zheng, Y. Distinct Bound of the Quantum Speed Limit via the Gauge Invariant Distance. *Phys. Rev. Lett.* **2019**, *123*, 180403. https://doi.org/10.1103/PhysRevLett.123.180403.
41. Sun, S.; Peng, Y.; Hu, X.; Zheng, Y. Quantum Speed Limit Quantified by the Changing Rate of Phase. *Phys. Rev. Lett.* **2021**, *127*, 100404. https://doi.org/10.1103/PhysRevLett.127.100404.
42. Hu, X.; Sun, S.; Zheng, Y. Quantum speed limit via the trajectory ensemble. *Phys. Rev. A* **2020**, *101*, 042107. https://doi.org/10.1103/PhysRevA.101.042107.
43. Czerwinski, A. Open quantum systems integrable by partial commutativity. *Phys. Rev. A* **2020**, *102*, 062423. https://doi.org/10.1103/PhysRevA.102.062423.
44. Zheng, L.; Peng, Y. Quantum decoherence of a two-level system in colored environments. *Phys. Rev. A* **2022**, *105*, 052443. https://doi.org/10.1103/PhysRevA.105.052443.
45. Lan, K.; Xie, S.; Cai, X. Geometric quantum speed limits for Markovian dynamics in open quantum systems. *New J. Phys.* **2022**, *24*, 055003. https://doi.org/10.1088/1367-2630/ac696b.
46. Czerwinski, A. Dynamics of Open Quantum Systems-Markovian Semigroups and Beyond. *Symmetry* **2022**, *14*, 1752. https://doi.org/10.3390/sym14081752.
47. Hadipour, M.; Haseli, S.; Dolatkhah, H.; Haddadi, S.; Czerwinski, A. Quantum Speed Limit for a Moving Qubit inside a Leaky Cavity. *Photonics* **2022**, *9*, 875. https://doi.org/10.3390/photonics9110875.
48. Schlosshauer, M. Decoherence, the measurement problem, and interpretations of quantum mechanics. *Rev. Mod. Phys.* **2005**, *76*, 1267. https://doi.org/10.1103/RevModPhys.76.1267.
49. Clerk, A.A.; Devoret, M.H.; Girvin, S.M.; Marquardt, F.; Schoelkopf, R.J. Introduction to quantum noise, measurement, and amplification. *Rev. Mod. Phys.* **2010**, *82*, 1155. https://doi.org/10.1103/RevModPhys.82.1155.
50. Gurvitz, S.A.; Fedichkin, L.; Mozyrsky, D.; Berman, G.P. Relaxation and the Zeno Effect in Qubit Measurements. *Phys. Rev. Lett.* **2003**, *91*, 066801. https://doi.org/10.1103/PhysRevLett.91.066801.
51. Kang, L.; Zhang, Y.; Xu, X.; Tang, X. Quantum measurement of a double quantum dot coupled to two kinds of environment. *Phys. Rev. B* **2017**, *96*, 235417. https://doi.org/10.1103/PhysRevB.96.235417.
52. Lan, K.; Du, Q.; Kang, L.; Tang, X.; Jiang, L.; Zhang, Y.; Cai, X. Dynamics of an open double quantum dot system via quantum measurement. *Phys. Rev. B* **2020**, *101*, 174302. https://doi.org/10.1103/PhysRevB.101.174302.
53. Silberfarb, A.; Jessen, P.S.; Deutsch, I.H. Quantum State Reconstruction via Continuous Measurement. *Phys. Rev. Lett.* **2005**, *95*, 030402. https://doi.org/10.1103/PhysRevLett.95.030402.
54. Smith, A.; Riofrío, C.A.; Anderson, B.E.; Sosa-Martinez, H.; Deutsch, I.H.; Jessen, P.S. Quantum state tomography by continuous measurement and compressed sensing. *Phys. Rev. A* **2013**, *87*, 030102. https://doi.org/10.1103/PhysRevA.87.030102.

55. Merkel, S.T.; Riofrío, C.A.; Flammia, S.T.; Deutsch, I.H. Random unitary maps for quantum state reconstruction. *Phys. Rev. A* **2010**, *81*, 032126. https://doi.org/10.1103/PhysRevA.81.032126.
56. Czerwinski, A. Quantum state tomography with informationally complete POVMs generated in the time domain. *Quantum Inf. Process.* **2021**, *20*, 105. https://doi.org/10.1007/s11128-021-03045-9.
57. Czerwinski, A. Selected Concepts of Quantum State Tomography. *Optics* **2022**, *3*, 268. https://doi.org/10.3390/opt3030026.
58. Heinosaari, T.; Ziman, M. *The Mathematical Language of Quantum Theory*; Cambridge University Press: Cambridge, UK, 2012.
59. Nielsen, M.A.; Chuang, I.L. *Quantum Computation and Quantum Information*; Cambridge University Press: Cambridge, UK, 2000.
60. Martens, C.C. Communication: Decoherence in a nonequilibrium environment: An analytically solvable model. *J. Chem. Phys.* **2010**, *133*, 241101. https://doi.org/10.1063/1.3507870.
61. Martens, C.C. Quantum dephasing of a two-state system by a nonequilibrium harmonic oscillator. *J. Chem. Phys.* **2013**, *139*, 024109. https://doi.org/10.1063/1.4811219.
62. Lombardo, F.C.; Villar, P.I. Nonunitary geometric phases: A qubit coupled to an environment with random noise. *Phys. Rev. A* **2013**, *87*, 032338. https://doi.org/10.1103/PhysRevA.87.032338.
63. Lombardo, F.C.; Villar, P.I. Correction to the geometric phase by structured environments: The onset of non-Markovian effects. *Phys. Rev. A* **2015**, *91*, 042111. https://doi.org/10.1103/PhysRevA.91.042111.
64. Cai, X.; Zheng, Y. Decoherence induced by non-Markovian noise in a nonequilibrium environment. *Phys. Rev. A* **2016**, *94*, 042110. https://doi.org/10.1103/PhysRevA.94.042110.
65. Cai, X.; Zheng, Y. Non-Markovian decoherence dynamics in nonequilibrium environments. *J. Chem. Phys.* **2018**, *149*, 094107. https://doi.org/10.1063/1.5039891.
66. Cai, X.; Zheng, Y. Quantum dynamical speedup in a nonequilibrium environment. *Phys. Rev. A* **2017**, *95*, 052104. https://doi.org/10.1103/PhysRevA.95.052104.
67. Lin, D.; Zou, H.M.; Yang, J. Based-nonequilibrium-environment non-Markovianity, quantum Fisher information and quantum coherence. *Phys. Scr.* **2019**, *95*, 015103. https://doi.org/10.1088/1402-4896/ab4012.
68. Cai, X.; Meng, R.; Zhang, Y.; Wang, L. Geometry of quantum evolution in a nonequilibrium environment. *Europhys. Lett.* **2019**, *125*, 30007. https://doi.org/10.1209/0295-5075/125/30007.
69. Basit, A.; Ali, H.; Badshah, F.; Yang, X.F.; Ge, G.Q. Controlling sudden transition from classical to quantum decoherence via non-equilibrium environments. *New J. Phys.* **2020**, *22*, 033039. https://doi.org/10.1088/1367-2630/ab76f6.
70. Basit, A.; Ali, H.; Badshah, F.; Yang, X.F.; Ge, G. Nonequilibrium effects on one-norm geometric correlations and the emergence of a pointer-state basis in the weak- and strong-coupling regimes. *Phys. Rev. A* **2021**, *104*, 042417. https://doi.org/10.1103/PhysRevA.104.042417.
71. Chen, M.; Chen, H.; Han, T.; Cai, X. Disentanglement Dynamics in Nonequilibrium Environments. *Entropy* **2022**, *24*, 1330. https://doi.org/10.3390/e24101330.
72. Tang, J.S.; Li, C.F.; Li, Y.L.; Zou, X.B.; Guo, G.C.; Breuer, H.P.; Laine, E.M.; .; Piilo, J. Measuring non-Markovianity of processes with controllable system-environment interaction. *Europhys. Lett.* **2012**, *97*, 10002. https://doi.org/10.1209/0295-5075/97/10002.
73. Cai, X. Quantum Dynamics in a Fluctuating Environment. *Entropy* **2019**, *21*, 1040. https://doi.org/10.3390/e21111040.
74. Fuliński, A. Non-Markovian noise. *Phys. Rev. E* **1994**, *50*, 2668. https://doi.org/10.1103/PhysRevE.50.2668.
75. Cai, X. Quantum dephasing induced by non-Markovian random telegraph noise. *Sci. Rep.* **2020**, *10*, 88. https://doi.org/10.1038/s41598-019-57081-8.
76. Wootters, W.K.; Fields, B.D. Optimal state-determination by mutually unbiased measurements. *Ann. Phys.* **1989**, *191*, 363. https://doi.org/10.1016/0003-4916(89)90322-9.
77. Yu, T.; Eberly, J.H. Finite-time Disentanglement via Spontaneous Emission. *Phys. Rev. Lett.* **2004**, *93*, 140404. https://doi.org/10.1103/PhysRevLett.93.140404.
78. Bellomo, B.; Lo Franco, R.; Compagno, G. Non-Markovian Effects on the Dynamics of Entanglement. *Phys. Rev. Lett.* **2007**, *99*, 160502. https://doi.org/10.1103/PhysRevLett.99.160502.
79. Nemoto, K. Generalized coherent states for SU(n) systems. *J. Phys. A* **2000**, *33*, 3493. https://doi.org/10.1088/0305-4470/33/17/307.
80. Bertlmann1, R.A.; Krammer, P. Bloch vectors for qudits. *J. Phys. A* **2008**, *41*, 235303. https://doi.org/110.1088/1751-8113/41/23/235303.